

## **Pore scale insights into estimations of residual gas saturation**

Pradeep Bhattad<sup>1</sup>, Alan A. Curtis<sup>1</sup>, Alex Mock<sup>2</sup>, Michael Turner<sup>3</sup>, Benjamin Young<sup>1</sup>,  
Anna Carnerup<sup>1</sup> and Mark Knackstedt<sup>1</sup>

(1) Lithicon Australia, Canberra, (2) Lithicon Norway, Trondheim, (3) Department of  
Applied Mathematics, Australian National University, Canberra

*This paper was prepared for presentation at the International Symposium of the Society of Core  
Analysts held in Napa Valley, California., USA, 16-19 September, 2013.*

### **ABSTRACT**

We study in detail the pore scale distribution and estimation of residual gas saturation ( $S_{gr}$ ) in an analogue tight reservoir experiencing water encroachment. Many studies have, based on empirical evidence, tried to understand gas-trapping mechanisms (e.g. influence of rock type, initial gas saturation, permeability) [1-6]. In particular, systematic deviations in  $S_{gr}$  prediction are observed and shown to depend on a number of parameters (e.g., pore geometry, mineralogy, reservoir quality) [1-3]. One particularly curious trend shows  $S_{gr}$  decreasing in poorer quality rocks [2,3]. Here we use pore scale mapping of residual gas saturation to help understand these empirical trends.

In this study we undertake 3D imaging experiments to directly observe the trapped gas at the pore scale and to correlate this to the pore/microporous structure, the mineral/clay composition and plug scale heterogeneity of conventional and tight gas sands. Four petrofacies types (good, medium, poor and laminated sands) are considered. The results of the flooding studies highlight the role of microporosity in controlling  $S_{gr}$ . A multi-resolution approach based on capturing the dominant microfacies, understanding properties for each facies class and using an upscaling routine to represent the plug scale properties is then briefly discussed. The results show a consistent match to available experiment.

The work demonstrates how insight into pore scale mechanisms can assist in understanding static and dynamic properties of tight reservoir core material.

### **INTRODUCTION**

Predicting the efficiency of the gas recovery by waterflood or capillary trapping of  $CO_2$  requires a better understanding of imbibition mechanisms at the pore scale. Most of the imbibition mechanisms have been derived from the direct observation of flow in the 2D glass micromodels. These experiments are ideally suited for visualizing the behaviour of interfaces in pores and throats; however they represent a simplistic pore space and do not capture the complex pore connectivity observed in the 3D porous rocks incorporating variable texture and mineralogy and the presence of fine grained regions, micro-porosity and clays.

Many experimental studies have reported end point saturations of gas recovery processes into sand-packs, sandstones and carbonate core plugs. It is reported that porosity, pore-network topology, clay content, micro-porosity, permeability had a strong influence; while temperature and pressure [9,10], displacement rates [9,11], formation and cementation factor [11] show weaker influence in the gas trapping ability. In some cases counterintuitive data is obtained—for example the observation that poorer quality rocks exhibit a lower  $S_{gr}$  [1-3,11]. In this paper we study this observation at a pore scale in 3D.

We use high resolution and non-destructive 3D micro-CT imaging techniques [4-6] to characterize the endpoint of a spontaneous imbibition in a complex pore space. We demonstrate the ability to directly observe the trapped gas at the pore scale and to correlate this to the pore/microporous structure, the mineral/clay composition and plug scale heterogeneity of conventional and tight gas sands.

## **EXPERIMENTAL**

Spontaneous imbibition experiments were carried out on four sandstone samples of varying quality representing good, medium, poor and laminated petrofacies types. Sub-plugs of (Diameter 3-5mm, Height 19mm) were extracted and cleaned to ensure strong water-wet conditions. Samples were imaged in the dry state prior to the spontaneous imbibition experiment. Air in pore-space was replaced by butane under vacuum and spontaneous imbibition experiments were carried out in a butane flushed chamber. The sub-plug was suspended from the balance, as shown in the Figure 1, and other end of the plug was brought in contact with a reservoir containing 0.15M CsI-H<sub>2</sub>O brine. Imbibition was stopped when a constant weight was reached and samples were imaged again in the imbibed state. To avoid end effects, approximately 5mm region from the middle of tall sub-plug image was considered in the analysis. Sister plugs of 8mm diameter were also extracted from each rock to obtain pore-size distribution from mercury injection (MICP) experiments (Figure 3).

On the laminated sandstone sub-plug further experiments (secondary drainage and imbibition) were carried out. The sample was dried and saturated with 1M CsI-H<sub>2</sub>O brine under vacuum to ensure complete saturation. Higher CsI concentration was used in this set of experiments to ensure sufficient X-ray contrast in the tomogram to capture the irreducible water saturation in the tighter rock matrix at the end of drainage. The sample was drained using a centrifuge under a butane rich atmosphere to 400 nm equivalent throat diameter. The sample was sealed and allowed to equilibrate for 24hrs before imaging. Secondary imbibition was then undertaken and the sample was imaged again.

## **RESULTS AND DISCUSSION**

3D micro-CT images acquired at various stages of the experiment (dry, imbibed, saturated and drained) were registered into a perfect geometric alignment. These images (Figure 2) allow one to clearly distinguish gas saturation from water and image registration along with the image segmentation enabled us to observe and quantify the distribution of the wetting phase and the non-wetting phase in the pore space.

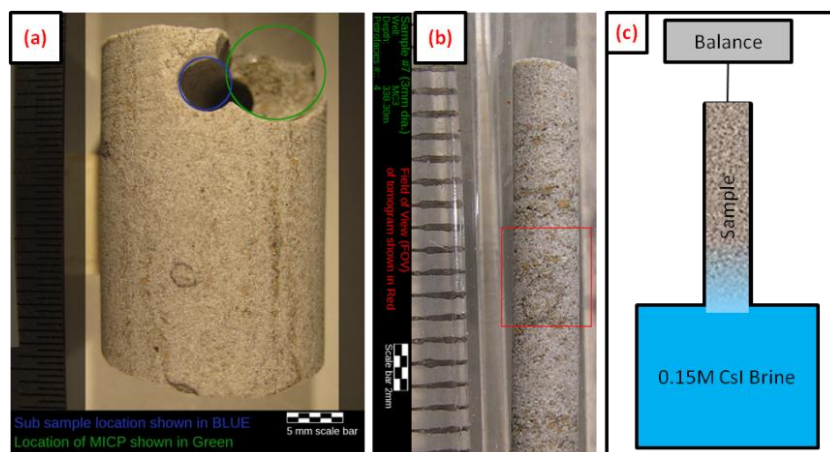


Figure 1. Photograph of sample 47L showing (a) 19mm plug with location of 3mm sub-plug extracted for imaging and sister 8mm sub-plug chosen for MICP, (b) 3mm sub-plug highlighting the region used in this study, and (c) experimental setup for spontaneous imbibition.

Variation of pore geometry between four rock types chosen for this study can be clearly seen from the dry tomograms (Figure 2) and MICP (Figure 3). In order to further quantify rock quality, permeability and formation factor simulations were also carried out on the segmented image. Higher formation factor values were observed for the tighter samples. Poro-perm trends also show the decrease in the permeability and porosity with the rock quality. Permeability results could not be simulated on the sample 47L because of connected pore space could not be resolved at the microCT resolution ( $1.73\mu\text{m}$ ) in the very tight lamellae. In our other work [12], we have developed a multiple scale imaging and simulation workflow for the prediction of the petrophysical and flow properties of tight reservoir sandstones. From the MICP drainage data one can determine the expected  $S_{wi}$  for each sample (assuming specific saturation: height/capillary pressure).  $S_{gi}$  values for primary imbibition (figure 4e) in the dry samples are estimated based on a the drainage pressure  $P_c=200$  psi (pore entry diameter = 485 nm). Values of  $S_{gr}$  show a strong trend of decreasing with rock decrease in rock quality and permeability. Good and medium quality sands show  $S_{gr}$  of ~30-50% while the tight lamina of sample 47L showed much lower  $S_{gr}$  (17%). These observations are consistent with the reported data [1-3]. Little to no gas trapping was observed in the micro-porous region and most of the gas trapped was in the large pores.

Figure 4b show the endpoint of spontaneous imbibition into a subset of the dry rock. The endpoint of spontaneous imbibition was also imaged after drainage to  $S_{wi}$  (Figure 4c) to study the effect of presence of wetting films, pendular rings and filled pores ahead of the bulk front. Figure 4d show 4% increase in  $S_{gr}$ . The increase in  $S_{gr}$  is due to the presence of films enhancing the potential for snap off of gas- in particular we observe enhanced trapping of gas in the clay rich regions of high porosity.

From the SEM of good quality sandstone 41G (Figure 5), we can see the pore structure of clay, which in contrast with the large open pores shows a very wide pore-throat size

distribution (note MICP data in Figure 3). Clay minerals were also identified in QEMScan (Figure 5c); however it is not possible to correlate mineralogy to gas trapping in this sample set.

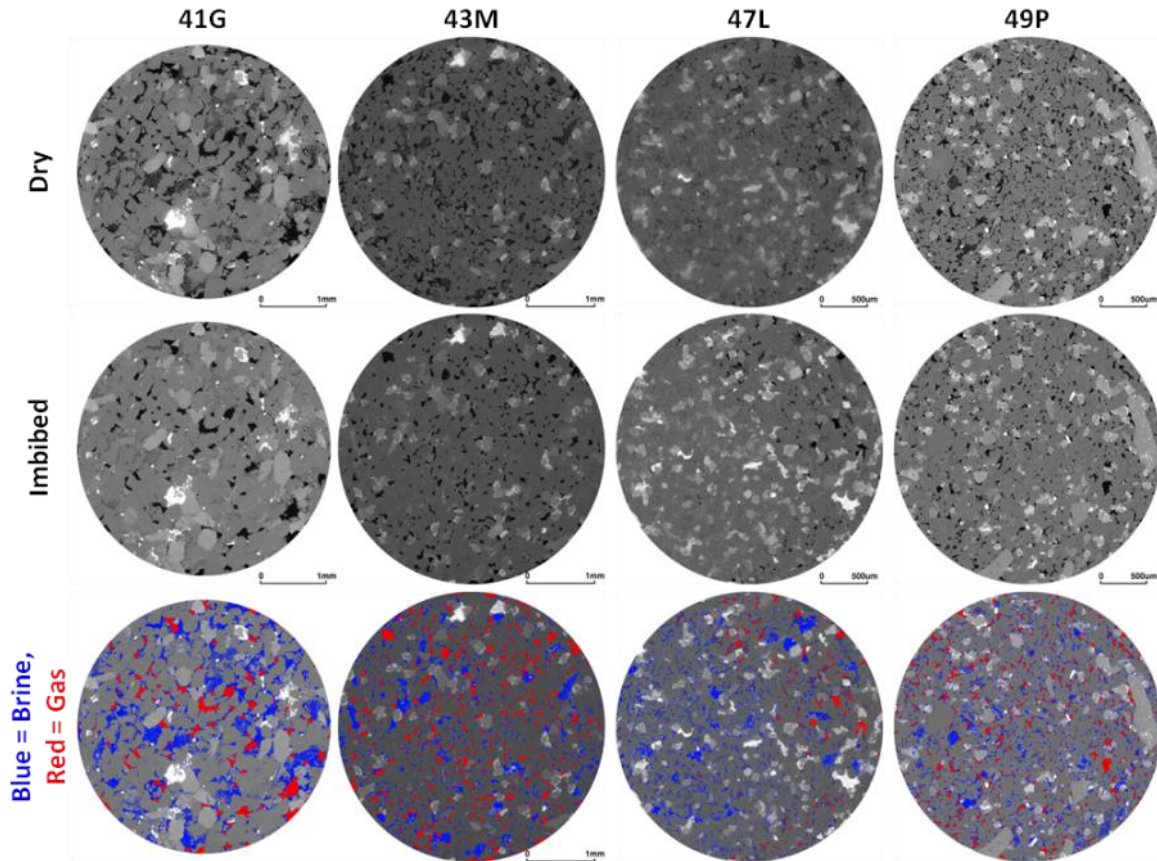


Figure 2. Slice of tomogram showing (Top) Dry, (Center) after primary imbibition and (Bottom) Overlay of segmented wetting phase (blue) and gas (red) obtained from the difference between the imbibed and dry tomograms. Image resolution  $1.7\mu\text{m}/\text{voxel}$

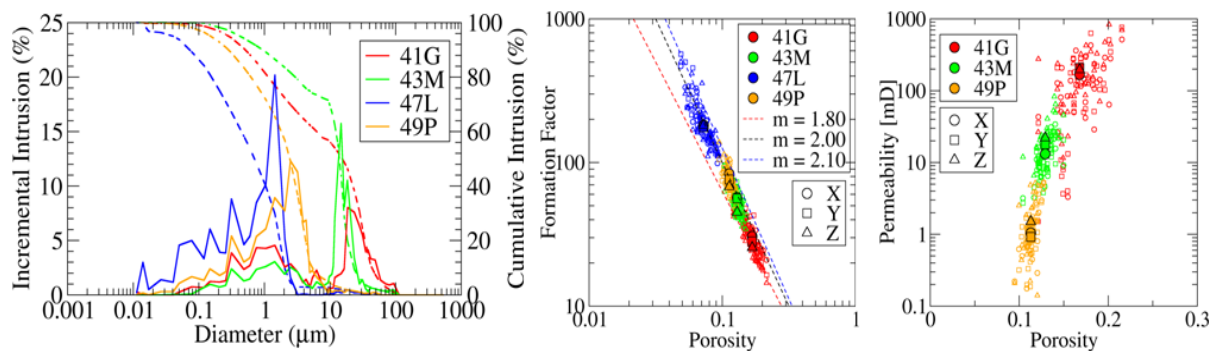


Figure 3. Petrophysical properties of four samples analysed. Left to Right: MICP on sister plugs, Formation factor vs porosity, and Permeability vs porosity (Permeability could not be calculated on 47L).

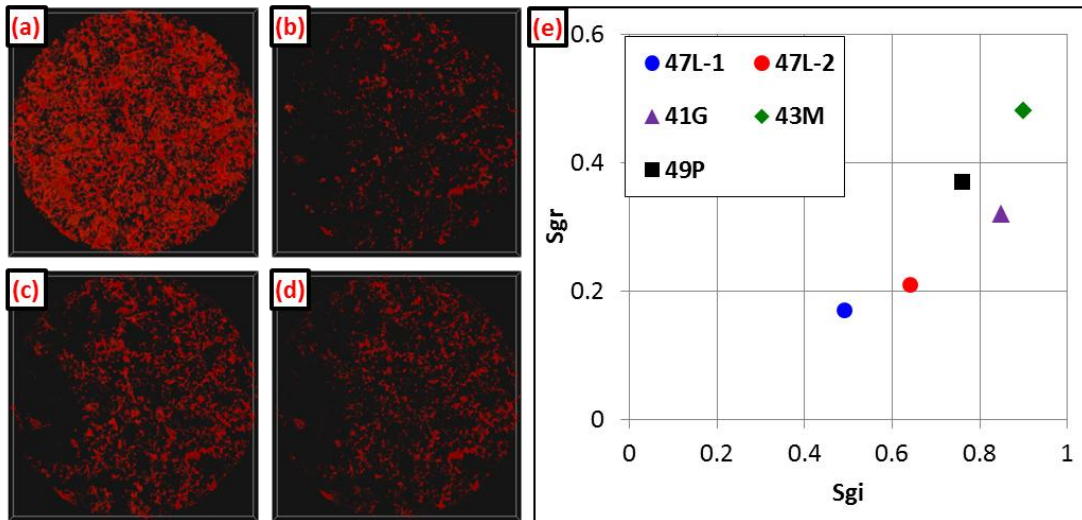


Figure 4. 3D Visualization of a small section ( $2.9 \times 2.9 \times 0.17 \text{ mm}^3$ ) of sample 47L, showing gas saturation at various stages of experiment. (a) Dry sample (porosity 7.4%), (b) Primary imbibition ( $S_{gr} = 0.17$ , 47L-1 in the graph), (c) drainage ( $S_{gi} = 0.36$ ), (d) secondary imbibition ( $S_{gr} = 0.21$ , 47L-2 in the graph), and (e)  $S_{gi}$  vs.  $S_{gr}$  relationship.

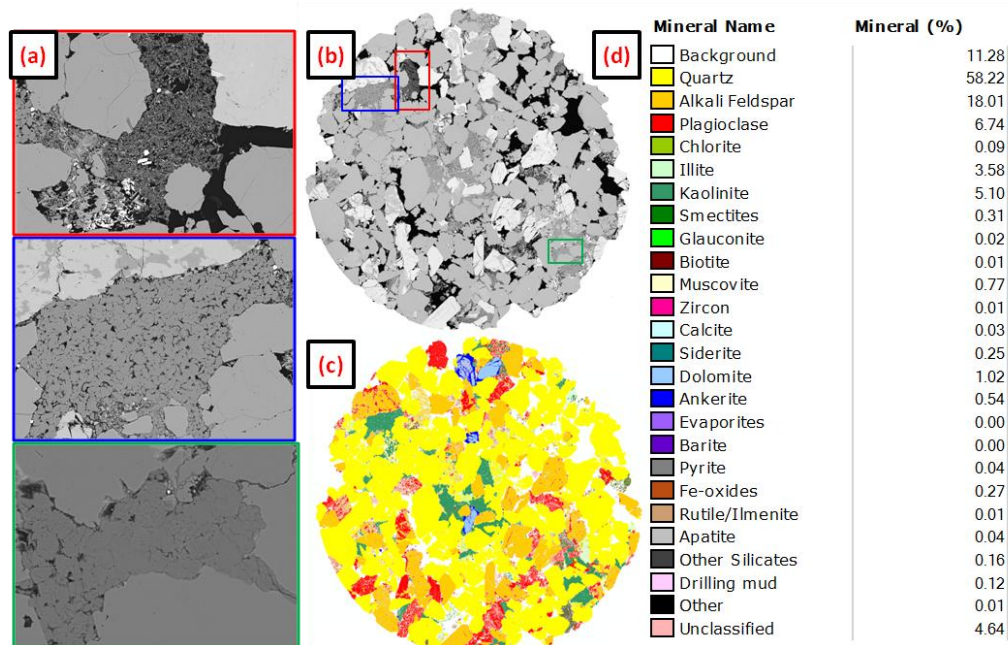


Figure 5. SEM and QEMscan prepared from an analogue sub-plug of sample 41G. (a) High resolution SEM showing clay micro-structure, (b) SEM showing entire plug, (c) QEM-scan showing mineralogy and (d) Mineralogy legend.

## CONCLUSION

Direct observation of the residual gas saturation using X-ray microCT is a powerful tool in furthering our understanding of multiphase displacement phenomena in the natural porous media. We observe that in tight sands the micro-porous clay region is mostly swept and the gas trapped is mainly in the large pores in the form of disconnected blobs

or ganglia spanning several pores. Gas trapping is enhanced with wider pore size distribution as was the case in the high porosity samples containing clay compared to the lower Sgr observed in the clay filled tight lamina with narrow pore size distribution. Decreasing trend in the gas trapping with decreasing rock quality is in good agreement with the published results for shaly sandstones. Effects of mineralogy could not be determined, since the samples were plasma treated to make sample strongly water wet. Increased gas trapping in the presence of films, also confirms trapping due to snap-off ahead of the bulk front for the same.

## REFERENCES

1. Hamon, G., K. Suzanne, J. Billiotte, and V. Trocme, "Field-Wide Variations of Trapped Gas saturation in Heterogeneous Sandstone Reservoirs," in *SPE Annual Technical Conference and Exhibition*, New Orleans, 2001.
2. Suzanne, K., G. Hamon, J. Billiotte, and V. Trocme, "Distribution of trapped gas saturation in heterogeneous sandstone reservoirs," in *International symposium of the Society of Core Analysts*, Edinburgh, 2001.
3. Suzanne, K., G. Hamon, J. Billiotte, and V. Trocme, "Experimental Relationships Between Residual Gas Saturation and Initial Gas Saturation in Heterogeneous Sandstone Reservoirs," in *SPE Annual Technical Conference*, Denver, 2003.
4. Kumar, M., M. Knackstedt, T. Senden, A. Sheppard, and J. Middleton, "Visualizing And Quantifying the Residual Phase Distribution In Core Material," *PetroPhysics*, vol. 51, 2010.
5. Pentland, C., S. Iglauer, O. Gharbi, K. Okada, and T. Suekane, "The Influence of Pore Space Geometry on the Entrapment of Carbon Dioxide by Capillary Forces," in *SPE Asia Pacific Oil and Gas Conference and Exhibition*, Perth, 2012.
6. Al-Raoush, R. and C. Willson, "A pore-scale investigation of a multiphase porous media system," *J. Contam. Hydrol.*, vol. 77, pp. 67–89, 2005.
7. Iglauer, S., W. Wulling, C. Pentland, S. Mansoori, and M. Blunt, "Capillary Trapping Capacity of Rocks and Sandpacks," in *EUROPEC/EAGE*, Amsterdam, 2009.
8. Lenormand, R., C. Zarcone, and A. Sarr, "Mechanisms of the displacement of one fluid by another in a network of capillary ducts," *J. Fluid Mech.*, vol. 135, pp. 337–353, 1983.
9. Geffen, T., D. Parrish, G. Haynes, and R. Morse, "Efficiency of Gas Displacement From Porous Media by Liquid Flooding," *J. Pet. Technol.*, vol. 4, pp. 29–38, 1952.
10. Chierici, G., G. Ciucci, and G. Long, "Experimental research on gas saturation behind the water front in gas reservoirs subjected to water drive," in *6th World Petroleum Congress*, Frankfurt, 1963.
11. Jerauld, G., "Prudhoe Bay Gas/Oil Relative Permeability," *Spe Reserv. Eng.*, vol. 12, 1997.
12. Long, H., C. Nardi, N. Idowu, A. Carnerup, P. Oren, M. Knackstedt, T. Varslot, R. Sok, "Study of Dry/wet Micro-CT Imaging to Capture Sub-resolution Microporosity in Sandstone," in *International symposium of the Society of Core Analysts*, California, 2013.